

Quantitative Oxygenation Venography from MRI Phase

Audrey Peiwen Fan¹, Berkin Bilgic¹, Louis Gagnon^{2,3}, Thomas Witzel³, Himanshu Bhat³, Bruce R Rosen^{2,3}, and Elfar Adalsteinsson^{1,3}

¹Electrical Engineering and Computer Science, Massachusetts Institute of Technology, Cambridge, MA, United States, ²Health Sciences and Technology, Harvard-MIT, Cambridge, MA, United States, ³Radiology, Athinoula A. Martinos Center for Biomedical Imaging, Charlestown, MA, United States

Target Audience. Physicians and scientists interested in quantitative evaluation of venous oxygenation in the brain.

Purpose. The ability to noninvasively image oxygenation would provide critical information to select patients for therapy in stroke and tumor [1]. MRI phase can be used to quantify oxygen saturation (SvO₂) in individual veins from the deoxyhemoglobin-induced susceptibility shift between vessels and brain tissue [2,3]. However, clinical application of phase-based SvO₂ imaging is limited by restrictions on vessel orientation that prevent general use of the technique across the brain. We address these limitations and demonstrate comprehensive venograms that map quantitative SvO₂ along each vessel.

Methods. Acquisition. We implemented a 3D gradient echo sequence with full flow-compensation along each axis at all echoes [4]. Axial images with magnitude and phase contrast were collected in three healthy volunteers with a 32-channel coil on a Siemens 3T Trio system (TR=14ms; TE=8.1, 20.3ms; resolution=0.6x0.6x0.6 mm³; matrix=384x336x176; BW=260Hz/pixel).

Susceptibility mapping. Phase images were spatially unwrapped with FSL Prelude [5] and background field was estimated by projection onto dipole fields for removal [6]. Unreliable phase voxels were identified as high spatial frequency structures in the estimated phase offset map at TE=0 and masked prior to QSM. Susceptibility (χ) maps were then reconstructed with ℓ_1 -regularization [7], which minimizes $\|F^H D F \chi - b\|_2^2 + \lambda \cdot |G\chi|_1$. Here, b is the measured local field map, $D=1/3 - k_z^2/k^2$ is the dipole kernel in k-space, G is the gradient operator, F is the Fourier transform, and $\lambda=2 \cdot 10^{-4}$ was chosen by an L-curve heuristic.

Vessel graphing. Reconstructed χ maps were thresholded at $\chi > 0.10$ to isolate veins for graphing with VIDA suite in Matlab [8] (Fig 1). A 3D mesh was created from the resulting graph structure, and $SvO_2 = 1 - \Delta\chi_{\text{vein-tissue}} / (0.27\text{ppm} \cdot Hct)$ at each node was displayed as the maximal value within a 2-mm radius of the node.

Results and Discussion. After graphing, the venous vasculature was represented by 1322 nodes and 1294 edges, covering 3.6m of total tracked vessel length, on average across subjects. Quantitative SvO₂ venograms were created for each volunteer, from which we identified major anatomical veins and the corresponding SvO₂ (%) for each vessel (Fig2).

In addition to venogram display, the graph structure enabled *in vivo* investigation of potential bias in SvO₂ estimate as a function of vessel tilt angle (θ) relative to the main field (B_0). This characterization is important because the dipole kernel undersamples Fourier data near the magic angle. We compared SvO₂ in vessels with tilt angles undersampled at $|D| < 0.15$ to values in parallel veins ($\theta < 25.4^\circ$) that are expected to exhibit minimal bias. In numerical simulation (Fig3a), we observed increased SvO₂ in undersampled ($69.5 \pm 2\%$) relative to parallel ($63.1 \pm 1\%$) orientations, $p < 10^{-3}$. A similar profile was observed *in vivo* (Fig3b), with the same finding of increased SvO₂ at undersampled ($69.6 \pm 1\%$) relative to parallel ($66.2 \pm 1\%$) tilt angles, $p < 10^{-3}$. This observation motivates future work to incorporate vessel angle priors from graphing into model-based reconstruction of more accurate SvO₂ venograms. The model could also integrate vessel diameter to mitigate partial volume effects on quantitative SvO₂.

Conclusion. Venograms which map oxygenation along each vessel are shown for the first time, and may facilitate clinical use of SvO₂ imaging.

References. [1] Christen, *Am J Neuroradiol* 2012. [2] Fan, *Magn Reson Med* 2012. [3] Haacke, *Human Brain Mapp* 1997. [4] Deistung, *J Magn Reson Imag* 2009. [5] Jenkinson, *Magn Reson Med* 2003. [6] Liu, *NMR Biomed* 2012. [7] Bilgic, *Neuroimage* 2011. [8] Tsai, *J Neurosci* 2009. **Funding:** NSF GRFP, R01-EB007942.

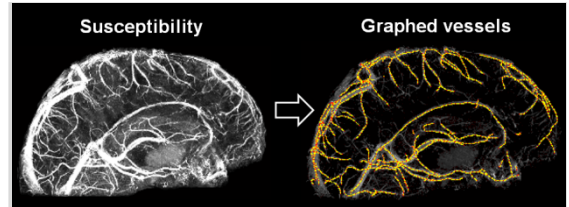
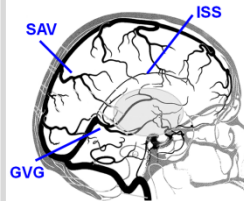
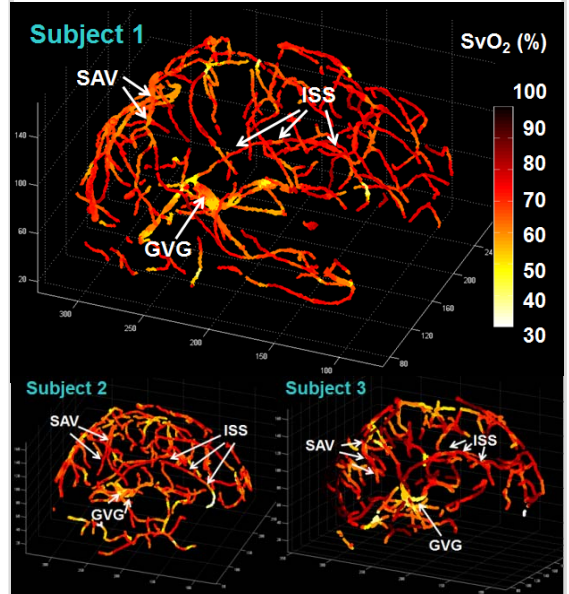


Fig1. Maximum intensity projection (60mm) of susceptibility map and graphed vasculature structure.



SvO ₂ (%)	S1	S2	S3
SAV	62.4	67.7	69.8
ISS	66.5	63.8	67.4
GVG	57.7	56.9	61.6

Fig2. Quantitative SvO₂ (%) venograms displayed on 3D mesh for three subjects, compared to schematic of venous drainage in the brain. *In vivo* SvO₂ values are tabulated for the superior anastomotic vein (SAV), inferior sagittal sinus (ISS) and the great vein of Galen (GVG).

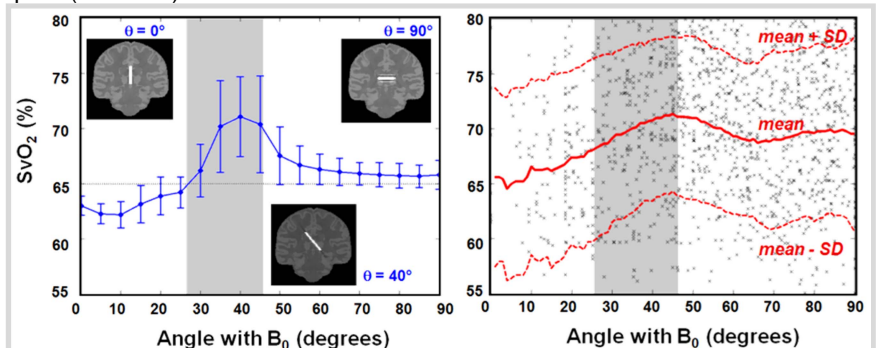


Fig3. (a) Numerical simulation of SvO₂ versus vessel tilt angle (true SvO₂= 65%). (b) Similar profile of SvO₂ versus tilt angle is observed *in vivo* from one subject. Shaded regions indicate vessel orientations undersampled at kernel threshold of $|D| < 0.15$.